

# $\eta_{c2}(^1D_2)$ and its electromagnetic decays

Xin-Yao Du<sup>1,2,3\*</sup>, Su-Yan Pei<sup>1,2,3</sup>, Wei Li<sup>1,2,3</sup>, Man  
Jia<sup>1,2,3</sup>, Qiang Li<sup>4</sup>, Tianhong Wang<sup>5</sup>, Guo-Li Wang<sup>1,2,3†</sup>

<sup>1</sup> *Department of Physics, Hebei University, Baoding 071002, China*

<sup>2</sup> *Hebei Key Laboratory of High-precision Computation and  
Application of Quantum Field Theory, Baoding 071002, China*

<sup>3</sup> *Hebei Research Center of the Basic Discipline  
for Computational Physics, Baoding 071002, China*

<sup>4</sup> *School of Physical Science and Technology,  
Northwestern Polytechnical University, Xi'an 710129, China*

<sup>5</sup> *School of Physics, Harbin Institute of Technology, Harbin 150001, China*

## Abstract

The spin-singlet state  $\eta_{c2}(^1D_2)$  has not been discovered in experiment and it is the only missing low-excited  $D$ -wave charmonium, so in this paper, we like to study its properties. Using the Bethe-Salpeter equation method, we obtain its mass as 3828.2 MeV and its electromagnetic decay widths as  $\Gamma[\eta_{c2}(1D) \rightarrow h_c(1P)\gamma] = 284$  keV,  $\Gamma[\eta_{c2}(1D) \rightarrow J/\psi\gamma] = 1.04$  keV,  $\Gamma[\eta_{c2}(1D) \rightarrow \psi(2S)\gamma] = 3.08$  eV, and  $\Gamma[\eta_{c2}(1D) \rightarrow \psi(3770)\gamma] = 0.143$  keV. We estimate its full width to be about 366 keV, and point out that the electromagnetic decay partial width is very sensitive to its mass and show the variation of the width along with the mass in the range of 3800 ~ 3872 MeV. In our calculation, the emphasis is put on the relativistic corrections. Our results show that  $\eta_{c2} \rightarrow h_c\gamma$  is the non-relativistic  $E1$  transition dominated  $E1 + M2 + E3$  decay, and  $\eta_{c2} \rightarrow \psi\gamma$  is the  $M1 + E2 + M3 + E4$  decay but the relativistic  $E2$  transition contributes the most.

---

\* duxinyao0401@163.com

† wgl@hbu.edu.cn, corresponding author

## I. INTRODUCTION

In the last two decades, the Belle, BaBar, BESIII, LHCb collaborations, etc., have discovered a large number of new charmonium-like states [1–10] that are above the charmonium threshold and many of which do not match with the predictions of the underlying model calculations based on the conventional hadron assumptions [11, 12]. These exotic hadrons are often referred to as “ $X, Y, Z$ ” particles, and have aroused great research interest. However, there are still some conventional low-excited charmonia that have not been discovered by experiments, such as the  $\eta_{c2}(1^1D_2)$  and  $\chi_{c2}(1^3F_2)$ , etc. The supplementation of these traditional mesons in the charmonium family is crucial for the success of traditional potential models and QCD theory.

In the charmonium family, there are four  $D$ -wave states, namely  $\psi(3^3D_1)$ ,  $\psi_2(3^3D_2)$ ,  $\psi_3(3^3D_3)$ , and  $\eta_{c2}(1^1D_2)$ , their quantum numbers are  $1^{--}$ ,  $2^{--}$ ,  $3^{--}$  and  $2^{-+}$ , respectively.  $\psi(1^3D_1)$ , also known as the  $\psi(3770)$ , was the first observed  $D$  wave charmonium because it can be produced directly in  $e^+e^-$  collisions [13]. Belle [14] and BESIII [15] observed the particle  $X(3823)$  by its transition  $X(3823) \rightarrow \gamma\chi_{c1}$  in  $B$  decay and  $e^+e^-$  annihilation, respectively. And it is found that  $X(3823)$  is a good candidate of  $\psi_2(1^3D_2)$  [16–18]. There is also a good candidate for  $\psi_3(1^3D_3)$  [19, 20], which is the recently observed particle  $X(3842)$  in experiment [21]. Currently,  $\eta_{c2}(1^1D_2)$  is the only missing low-excited  $D$  wave charmonium. Therefore, in this article, we will study the properties of the  $\eta_{c2}(1^1D_2)$ .

In 2003, a narrow resonant state  $X(3872)$  was discovered by the Belle collaboration [1], and  $\eta_{c2}(1^1D_2)$  was once assigned to this particle. However, theoretical calculations strongly contradict experimental data on the electromagnetic decay of  $X(3872)$  [22–24], and the quantum number of  $X(3872)$  was finally determined as  $J^{PC} = 1^{++}$  [25, 26]. In 2020, Belle Collaboration searched for  $\eta_{c2}(1^1D_2)$  within the mass range of  $3795 \sim 3845$  MeV in channels of  $B^+ \rightarrow \eta_{c2}(1^1D_2)K^+$ ,  $B^0 \rightarrow \eta_{c2}(1^1D_2)K_S^0$ ,  $B^0 \rightarrow \eta_{c2}(1^1D_2)\pi^-K^+$  and  $B^+ \rightarrow \eta_{c2}(1^1D_2)\pi^+K_S^0$  [27]. After that, Belle Collaboration also looked for  $\eta_{c2}(1^1D_2)$  in the mass range of  $3.8 \sim 3.88$  GeV in the process of  $e^+e^- \rightarrow \gamma\eta_{c2}(1^1D_2)$  [28]. Unfortunately, no  $\eta_{c2}(1^1D_2)$  signal was observed.

In theory,  $\eta_{c2}(1^1D_2)$  is estimated to have a mass of 3.80 to 3.88 GeV [29], between the

$D\bar{D}$  and  $D^*\bar{D}$  thresholds. As can be seen from parity conservation, its decay into  $D\bar{D}$  is forbidden. Therefore,  $\eta_{c2}(1^1D_2)$  is a narrow resonance state, and its main decay modes are strong decays to  $gg$ ,  $\eta_c\pi\pi$  [30–33] and electromagnetic (EM) decays [12, 34]. It is found that the process of  $\eta_{c2}(1^1D_2) \rightarrow h_c(1P)\gamma$  has the biggest branching ratio, so studying its EM radiative transitions is crucial for revealing the properties of  $\eta_{c2}(1^1D_2)$ . And the EM decays of  $\eta_{c2}(1^1D_2)$  have been studied by many models, such as the potential models [12, 33, 35], the light front quark model [23], the lattice QCD [36], and the non-relativistic models [18, 24, 37, 38], etc. However, in existing studies, people mainly focus on the greatest contribution, such as the electric dipole  $E1$  transition, and relativistic correction has not been carefully considered. And we have found that the relativistic corrections are relatively large for  $P$ -wave and  $D$ -wave charmonia, which cannot be ignored [39].

So in this paper, we will provide a relativistic study on the radiative EM decays of  $\eta_{c2}(1^1D_2)$  adopting the instantaneous Bethe-Salpeter (BS) method. The BS equation is a relativistic dynamic equation used to describe a two-body bound state in quantum field theory [40], and its instantaneous approximation is the Salpeter equation [41] which is suitable for heavy mesons. In our method, we construct the universal wave function of a meson according to its quantum number of  $J^{P(C)}$ , where 4 or 8 radial wave functions are unknown and are obtained numerically by solving the complete Salpeter equation. The relativistic wave function obtained in this way contains rich information, besides the main waves, all the meson wave functions contain other partial waves [42], which mainly contribute to the relativistic corrections. We will study the contributions of all the partial waves in detail in the main text. Besides the relativistic corrections, our method has been proven effective in many aspects, such as being able to explain the ‘1/2 vs 3/2’ puzzle [43]. In the study of radiative EM transitions, this method is also very powerful [44, 45] because we not only calculate the leading order contribution, but also provide a complete calculation that includes the transitions of  $E1 + M2 + E3 + \dots$  or  $M1 + E2 + M3 + \dots$  [16, 19, 46].

Another special benefit of this method is that we can provide the correct mass splitting between the  $2^{--}$  and  $2^{-+}$  states. Since the mass of the  $2^{--}$  state  $\psi_2(1^3D_2)$  has already been detected in the experiment, using it as an input parameter, we can provide a relatively reliable mass prediction of  $2^{-+}$  state  $\eta_{c2}(1^1D_2)$ . Therefore, in this article, we will study

the mass spectra of  $2^{-+}$  states as well as the  $2^{--}$  states. For the radiative EM decays of  $\eta_{c2}(1^1D_2)$ , we will focus on the main decay mode  $\eta_{c2}(1^1D_2) \rightarrow h_c(1P)\gamma$ , in addition, the decays to  $\psi(1S)\gamma$ ,  $\psi(2S)\gamma$  and  $\psi(3770)\gamma$  final states are also calculated, and the full decay width of  $\eta_{c2}(1^1D_2)$  is estimated. The relativistic corrections and behaviors of different partial waves are discussed. Finally, we present the behavior of the EM decay widths of  $\eta_{c2}(1^1D_2)$  as a function of its mass in the range of 3800~3872 MeV.

This paper is organized as follows, In Sec. II, we first show the method of calculating the transition amplitude of the EM decay. Then we provide the relativistic wave functions used in this paper, including their diagrams. The mass spectra of  $2^{--}$  and  $2^{-+}$  charmonia as well as the form factors are also given in this section. In Sec. III, we give the results of the EM decays, the discussions and conclusion.

## II. THE THEORETICAL CALCULATIONS

### A. Transition amplitude of EM decay

We take the decay channel  $\eta_{c2}(1^1D_2) \rightarrow \psi(^3S_1)\gamma$  as an example to show our method how to calculate the transition amplitude. In Figure 1, we show the Feynman diagrams for the radiative EM transition of  $\eta_{c2} \rightarrow \psi\gamma$ , and the corresponding transition amplitude can be written as

$$\langle \psi(P_f, \epsilon_f)\gamma(k, \epsilon_0) | \eta_{c2}(P, \epsilon_i) \rangle = (2\pi)^4 \delta^4(P - P_f - k) \epsilon_{0\xi} \mathcal{M}^\xi, \quad (1)$$

where  $\epsilon_0$  is the polarization vector of the emitting photon, while  $\epsilon_i$  and  $\epsilon_f$  are the polarization vectors of the initial and final mesons, respectively.  $P$ ,  $P_f$  and  $k$  are the momenta of the initial meson, final meson and final photon, respectively.

Fig. 1 shows that the Feynman diagrams of EM transition consist of two parts, where photons are emitted from quark and anti-quark, respectively. And the corresponding hadronic matrix element  $\mathcal{M}^\xi$  can be written as the overlapping integral over the wave functions of initial and final mesons [47]

$$\mathcal{M}^\xi = \int \frac{d^3q_\perp}{(2\pi)^3} Tr \left[ Q_1 e \frac{\not{P}}{M} \bar{\varphi}_f^{++}(q_\perp + \alpha_2 P_{f\perp}) \gamma^\xi \varphi_i^{++}(q_\perp) \right]$$

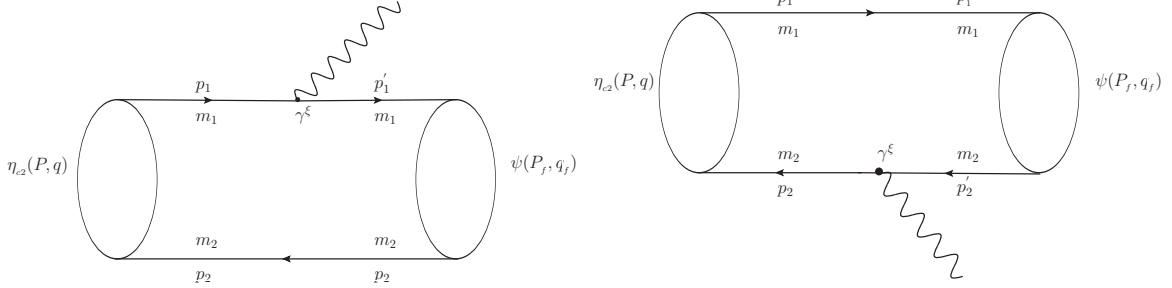


FIG. 1: Feynman diagrams for the EM transition of  $\eta_{c2} \rightarrow \psi\gamma$ .

$$+Q_2 e \bar{\varphi}_f^{++}(q_\perp - \alpha_1 P_{f\perp}) \frac{\not{P}}{M} \varphi_i^{++}(q_\perp) \gamma^\xi], \quad (2)$$

where  $q$  is the relative momentum between quark and antiquark. We have defined  $q_\perp = q - \frac{P \cdot q}{M^2} P$  and  $P_{f\perp} = P_f - \frac{P \cdot P_f}{M^2} P$ .  $\alpha_i = \frac{m_i}{m_1 + m_2}$  ( $i = 1, 2$ ),  $m_1$ ,  $m_2$ , and  $M$  are the masses of the quark, antiquark, and the initial meson, respectively.  $Q_1 e$  and  $Q_2 e$  are the charges of quark and anti-quark, respectively. We use subscript  $i$  representing the initial state and  $f$  the final state, so  $\varphi_i^{++}$  and  $\varphi_f^{++}$  are the positive energy wave functions of the initial and final mesons, respectively.

## B. The relativistic wave functions and the mass of $2^-$ state

In this paper, the relativistic wave functions are obtained by solving the instantaneous BS equation, namely the complete Salpeter equation. First, we provide the general representation of the relativistic wave function of a meson according to its quantum number of  $J^P$  or  $J^{PC}$ , where the radial wave functions are unknown,  $J$ ,  $P$  and  $C$  represent total angular momentum, the parity, and charge conjugate parity, respectively. Second, substitute this wave function into the Salpeter equation for solution, and obtain the numerical values of the radial wave functions. For simplicity, we will not introduce the BS equation and the Salpeter equation here, the interested readers are referred to the original papers [40, 41] or our previous articles, for example, Ref. [48].

1. *Mass and wave function of  $2^-$  state*

The general relativistic wave function for a  $2^-$  meson in the instantaneous approach can be written as [42]

$$\begin{aligned} \varphi_{2^-}(q_\perp) = & \epsilon_{\mu\nu} q_\perp^\mu q_\perp^\nu \left( a_1 + \frac{\not{P}}{M} a_2 + \frac{\not{q}_\perp}{M} a_3 + \frac{\not{P}\not{q}_\perp}{M^2} a_4 \right) \gamma^5 \\ & + \frac{i \epsilon_{\mu\nu\alpha\beta} \gamma^\mu P^\nu q_\perp^\alpha \epsilon^{\beta\delta} q_{\perp\delta}}{M} \left( i_1 + \frac{\not{P}}{M} i_2 + \frac{\not{q}_\perp}{M} i_3 + \frac{\not{P}\not{q}_\perp}{M^2} i_4 \right), \end{aligned} \quad (3)$$

where  $\epsilon_{\mu\nu}$  is the polarization tensor of the  $2^-$  state, and  $\epsilon_{\mu\nu\alpha\beta}$  is the Levi-Civita symbol.  $a_i$  and  $i_i$  ( $i = 1, 2, 3, 4$ ) are the radial wave functions, and they are function of  $-q_\perp^2$ . Not all the radial wave functions are independent, only half of them are, and according to the Salpeter equation, we have the relations

$$\begin{aligned} a_3 &= -a_1 \frac{M(\omega_1 - \omega_2)}{m_1\omega_2 + m_2\omega_1}, \quad a_4 = -a_2 \frac{M(\omega_1 + \omega_2)}{m_1\omega_2 + m_2\omega_1}, \\ i_3 &= i_1 \frac{M(\omega_1 - \omega_2)}{m_1\omega_2 + m_2\omega_1}, \quad i_4 = i_2 \frac{M(\omega_1 + \omega_2)}{m_1\omega_2 + m_2\omega_1}, \end{aligned}$$

where  $\omega_1 = \sqrt{m_1^2 - q_\perp^2}$  and  $\omega_2 = \sqrt{m_2^2 - q_\perp^2}$  are the energies of quark 1 and antiquark 2, respectively.

It can be checked that each term in Eq.(3) has a quantum number of  $2^-$ . With this wave function form as input, we solve the corresponding Salpeter equation and obtain the eigenvalues and the numerical values of the radial wave functions of all the  $2^-$  states [42], including the charmonia. That is to say, when the input masses of quark and antiquark are equal and both are charm quark mass, the system corresponds to charmonia. At this point, the solutions given by the Salpeter equation include both  $2^{--}$  and  $2^{-+}$  states. The first and second solutions are both ground  $1D$  states because the radial wave functions have no nodes. And the wave function of the first solution contains only non-zero  $i_i$  terms (except  $i_3 = 0$ ), while all  $a_i$  terms are zero, so it corresponds to the  ${}^3D_2$   $2^{--}$  state. The second solution is opposite to the first one, as its wave function only contains  $a_i$  terms (except  $a_3 = 0$ ) and all  $i_i$  terms are zero, therefore it is the  ${}^1D_2$   $2^{-+}$  state. The third and fourth solutions are similar to the first and second ones, corresponding to  $2^{--}$  and  $2^{-+}$  states, respectively, but they both have one node in their wave functions, so they are excited  $2D$  states, etc.

In our calculations, there are some parameters, such as quark mass, etc. To determine these parameters, the mass of the first solution is our input. Fortunately, the mass of the ground  $2^{-+}$  state is slightly higher than that of the  $2^{--}$  state in our model, and the ground  $2^{--}$  state  $X(3823)$  has been found in experiment [14, 15], so we can predict the ground mass of  $2^{-+}$  state successfully. Our predictions of mass spectra of  $2^{--}$  and  $2^{-+}$  charmonia are shown in Table I, where the ground mass of  $2^{--}$  state, 3823.0 MeV, is input, and the predicted mass of ground  $2^{-+}$  charmonium is 3828.2 MeV. The diagrams of independent radial wave functions  $a_1$  and  $a_2$  for the ground  $2^{-+}$  charmonium are shown in Figure 2.

TABLE I: Our predictions of the mass spectra of  $2^{--}$  and  $2^{-+}$  charmonium in unit of MeV

	$2^{--}$	$2^{-+}$
1D	3823.0 (input)	3828.2
2D	4153.7	4157.7
3D	4407.5	4410.7

The relativistic positive energy wave function for the  $2^{-+}$  state can be expressed as [30]

$$\varphi_{2^{-+}}^{++}(q_{\perp}) = \epsilon_{\mu\nu} q_{\perp}^{\mu} q_{\perp}^{\nu} \left[ A_1 + \frac{\not{P}}{M} A_2 + \frac{\not{P} \not{q}_{\perp}}{M^2} A_3 \right] \gamma^5, \quad (4)$$

where  $A_i$  are related to the original radial wave functions  $a_i$ ,

$$A_1 = \frac{1}{2} \left( a_1 + \frac{\omega_1}{m_1} a_2 \right), \quad A_2 = \frac{m_1}{2\omega_1} \left( a_1 + \frac{\omega_1}{m_1} a_2 \right), \quad A_3 = -\frac{A_2 M}{m_1},$$

where  $\omega_1 = \omega_2$ , and  $m_1 = m_2$  have been used.

As a relativistic method, the wave functions contain wealthy information. First, in the non-relativistic limit, there are no  $a_3$  and  $a_4$  terms in Eq.(3), so they are relativistic corrections, while  $a_1$  and  $a_2$  terms are non-relativistic. However, in our method, unlike other non-relativistic methods, they are independent and not equal, that is,  $a_1 \neq a_2$ , see Fig. 2. Second, it can be seen that the terms  $a_1$  and  $a_2$  in Eq.(3), or  $A_1$  and  $A_2$  terms in Eq.(4) are  $D$ -wave, but the  $a_3$  and  $a_4$  terms, or  $A_3$  term, are  $F$ -wave.

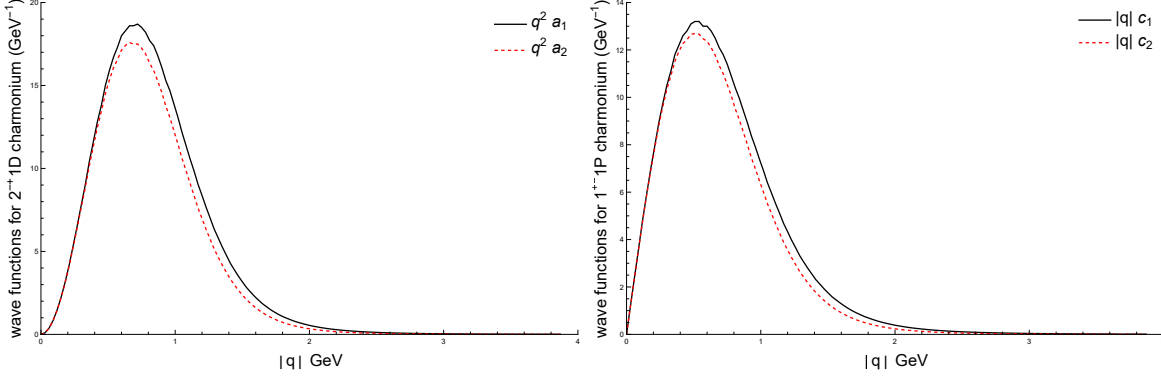


FIG. 2: The radial wave functions of the ground  $2^{-+}$  and  $1^{+-}$  charmonia.

## 2. Wave function of $1^{--}$ state

The positive energy wave function of the final state  $1^{--}$  is expressed as [49],

$$\begin{aligned} \varphi_{1^{--}}^{++}(q_{f\perp}) = & (\epsilon_f \cdot q_{f\perp}) \left[ B_1 + \frac{\not{P}_f}{M_f} B_2 + \frac{\not{q}_{f\perp}}{M_f} B_3 + \frac{\not{P}_f \not{q}_{f\perp}}{M_f^2} B_4 \right] \\ & + M_f \not{\epsilon}_f \left[ B_5 + \frac{\not{P}_f}{M_f} B_6 + \frac{\not{P}_f \not{q}_{f\perp}}{M_f^2} B_7 \right], \end{aligned} \quad (5)$$

where  $\epsilon_f$  is the polarization vector of the meson;  $B_i (i = 1, 2, \dots, 7)$  is a function of the four independent radial wave functions  $b_3, b_4, b_5$  and  $b_6$  of the  $1^{--}$  state, whose numerical values are obtained by solving the corresponding Salpeter equation [49], and we have,

$$\begin{aligned} f &= \frac{1}{2} \left( b_3 + \frac{m_f}{w_f} b_4 \right), \quad B_1 = \frac{q_{f\perp}^2}{M_f m_f} f + \frac{M_f}{2m_f} \left( b_5 - \frac{m_f}{w_f} b_6 \right), \quad B_5 = \frac{1}{2} \left( b_5 - \frac{w_f}{m_f} b_6 \right), \\ B_2 &= -\frac{M_f}{w_f} B_5, \quad B_3 = f - \frac{M_f^2}{2m_f w_f} b_6, \quad B_4 = \frac{w_f}{m_f} f - \frac{M_f^2}{2m_f w_f} b_5, \quad B_6 = -\frac{m_f}{w_f} B_5, \quad B_7 = B_2, \end{aligned}$$

where  $m_f = m_1$  and  $w_f$  are the mass and energy of the quark, respectively. In the wave function of Eq. (5), the terms including  $B_5$  and  $B_6$  are  $S$ -wave, the  $B_1, B_2$ , and  $B_7$  terms are  $P$ -wave, while  $B_3$  and  $B_4$  terms are  $D$ -wave mixed with  $S$ -wave, because

$$(\epsilon_f \cdot q_{f\perp}) \not{q}_{f\perp} = \frac{1}{3} q_{f\perp}^2 \not{\epsilon}_f + \left[ (\epsilon_f \cdot q_{f\perp}) \not{q}_{f\perp} - \frac{1}{3} q_{f\perp}^2 \not{\epsilon}_f \right], \quad (6)$$

where  $\frac{1}{3} q_{f\perp}^2 \not{\epsilon}_f$  is  $S$ -wave and  $(\epsilon_f \cdot q_{f\perp}) \not{q}_{f\perp} - \frac{1}{3} q_{f\perp}^2 \not{\epsilon}_f$  is  $D$ -wave. So in Eq. (5), the pure  $S$ -wave is

$$M_f \not{\epsilon}_f \left[ B_5 + \frac{\not{P}_f}{M_f} B_6 \right] + \frac{1}{3} q_{f\perp}^2 \not{\epsilon}_f \left[ \frac{1}{M_f} B_3 - \frac{\not{P}_f}{M_f^2} B_4 \right], \quad (7)$$



and the pure  $D$ -wave is

$$\left[ \epsilon_f \cdot q_{f\perp} \not{q}_{f\perp} - \frac{1}{3} q_{f\perp}^2 \not{\epsilon}_f \right] \left[ \frac{1}{M_f} B_3 - \frac{\not{P}_f}{M_f^2} B_4 \right]. \quad (8)$$

Since the expression of Eq.(5) is a general relativistic form for the wave function of  $1^{--}$  state, with this as input, as a relativistic dynamic equation for bound state, the solution of the Salpeter equation includes all possible  $1^{--}$  states, including states dominated by  $S$ -waves and states dominated by  $D$ -waves. We show the diagrams of the independent radial wave functions of the first three solutions in Figure 3. It can be seen that the wave functions of the ground state and the first excited state are dominant by  $S$ -waves, and their eigenvalues are 3096.9 MeV and 3688.1 MeV, so they are  $J/\psi$  and  $\psi(2S)$ , respectively. The second excited state is dominated by  $D$ -waves and there are no nodes in the wave functions, and its predicted mass is 3778.9 MeV, so it is the particle of  $\psi(3770)$  [50].

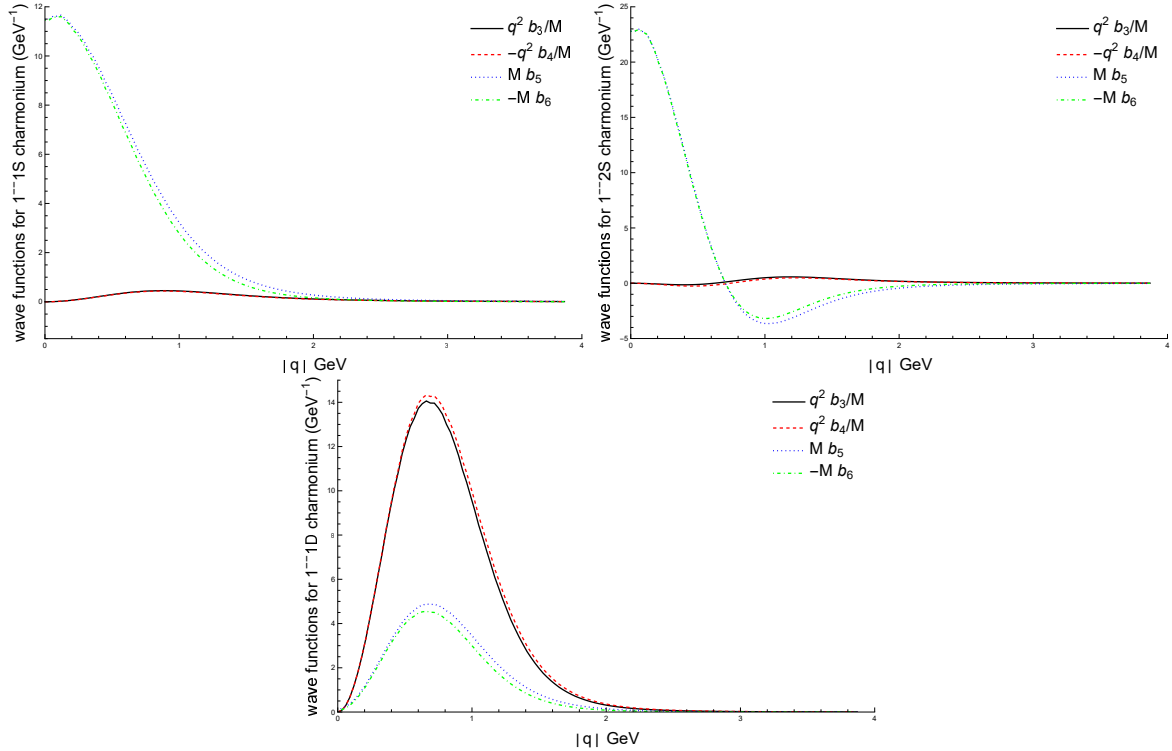


FIG. 3: The radial wave functions for the ground, first excited and second excited  $1^{--}$  states.

### 3. Wave function of $1^{+-}$ state

The positive energy wave function of the final state  $1^{+-}$  can be expressed as [51],

$$\varphi_{1^{+-}}^{++}(q_{f\perp}) = (\epsilon_f \cdot q_{f\perp}) \left[ C_1 + \frac{\not{P}_f}{M_f} C_2 + \frac{\not{P}_f \not{q}_{f\perp}}{M_f^2} C_3 \right] \gamma^5, \quad (9)$$

where the  $C_i$  are related to the original radial wave functions  $c_i$

$$C_1 = \frac{1}{2} \left( c_1 + \frac{w_f}{m_f} c_2 \right), \quad C_2 = \frac{1}{2} \left( \frac{m_f}{w_f} c_1 + c_2 \right), \quad C_3 = -\frac{M_f}{w_f} C_1,$$

and we show the diagrams of independent radial wave functions  $c_1$  and  $c_2$  in the right part of Fig.2. The mass of ground  $1^{+-}$  charmonium  $h_c(1P)$  is 3525 MeV. We also note that in Eq. (9), the terms including  $C_1$  and  $C_2$  are  $P$ -wave, and the  $C_3$  term is  $D$ -wave.

### C. The form factors

For  $\eta_{c2} \rightarrow \psi\gamma$ , we substitute Eq.(4) and Eq.(5) into Eq.(2), after integrate the internal momentum  $q_\perp$  over the initial and final state wave functions, we obtain the EM transition matrix element represented by the form factors,

$$\begin{aligned} \mathcal{M}_{2^{-+} \rightarrow 1^{--}}^\xi &= 2\varepsilon^{\xi P P_f \nu} \epsilon_{\nu P_f} P \cdot \epsilon_f t_1 + 2\varepsilon^{\xi P P_f \nu} \epsilon_{\nu \epsilon_f} t_2 + 2\varepsilon^{\xi \epsilon_f P \nu} \epsilon_{\nu P_f} t_3 \\ &+ 2\varepsilon^{\xi \epsilon_f P_f \nu} \epsilon_{\nu P_f} t_4 + \varepsilon^{\xi \epsilon_f P P_f} \epsilon_{P_f P_f} t_5 + 2P^\xi \varepsilon^{\epsilon_f P P_f \nu} \epsilon_{\nu P_f} t_6, \end{aligned} \quad (10)$$

where  $t_i$  ( $i = 1, 2 \dots 6$ ) is the form factor. And we have used some abbreviations here, for examples,  $\varepsilon^{\xi P P_f \nu} \equiv \varepsilon^{\xi \alpha \beta \nu} P_\alpha P_{f\beta}$  and  $\epsilon_{P_f P_f} = \epsilon_{\alpha\beta} P_f^\alpha P_f^\beta$ .

Similarly, for  $\eta_{c2} \rightarrow h_c \gamma$ , we insert Eq.(4) and Eq.(9) into Eq.(2), and obtain

$$\begin{aligned} \mathcal{M}_{2^{-+} \rightarrow 1^{+-}}^\xi &= P^\xi \epsilon_{P_f P_f} P \cdot \epsilon_f s_1 + P_f^\xi \epsilon_{P_f P_f} P \cdot \epsilon_f s_2 + 2\epsilon^{\xi P_f} P \cdot \epsilon_f s_3 \\ &+ 2P^\xi \epsilon_{P_f \epsilon_f} s_4 + 2P_f^\xi \epsilon_{P_f \epsilon_f} s_5 + \epsilon_f^\xi \epsilon_{P_f P_f} s_6 + 2\epsilon^{\xi \epsilon_f} s_7, \end{aligned} \quad (11)$$

where  $s_i$  ( $i = 1, 2 \dots 7$ ) is the form factor. Since the expressions of form factors  $t_i$  and  $s_i$  are very complex, we will not show the details.

For EM transition, we note that not all form factors are independent. Due to the gauge invariant condition  $(P_\xi - P_{f\xi})\mathcal{M}^\xi = 0$ , they satisfy the following constraints,

$$\begin{aligned} t_3 &= (M^2 - ME_f)t_6 - t_4, \\ s_6 &= (ME_f - M^2)s_1 - (ME_f - M_f^2)s_2 + 2s_3, \\ s_7 &= (M^2 - ME_f)s_4 + (ME_f - M_f^2)s_5. \end{aligned} \tag{12}$$

### III. NUMERICAL RESULTS AND DISCUSSIONS

In our calculation, the charm quark mass is chosen as  $m_c = 1.62$  GeV, and all the meson masses used have been mentioned in the text, for example, the predicted mass of  $\eta_{c2}(^1D_2)$  is 3828.2 MeV.

#### A. EM decay width of the $\eta_{c2}(^1D_2)$

As a  $2^{-+}$  state, the main EM decay of  $\eta_{c2}(^1D_2)$  is  $\eta_{c2}(^1D_2) \rightarrow h_c(1P)\gamma$ , which is mainly an  $E1$  transition. In our calculation, due to the use of relativistic wave functions, our result includes not only the non-relativistic  $E1$  transition, but also the relativistic  $M2$  and  $E3$  transitions [16], see Sec.III.B. Our result is

$$\Gamma [\eta_{c2}(^1D_2) \rightarrow h_c(1P)\gamma] = 284 \text{ keV}. \tag{13}$$

The  $\eta_{c2}(^1D_2)$  can also decay to a  $1^{--}$  charmonium, which is a  $M1$  transition in a non-relativistic method, but is  $M1 + E2 + M3 + \dots$  in our relativistic method. There are three channels of such decays, and our predictions are

$$\Gamma [\eta_{c2}(^1D_2) \rightarrow J/\psi\gamma] = 1.04 \text{ keV}, \tag{14}$$

$$\Gamma [\eta_{c2}(^1D_2) \rightarrow \psi(2S)\gamma] = 3.08 \text{ eV}, \tag{15}$$

$$\Gamma [\eta_{c2}(^1D_2) \rightarrow \psi(3770)\gamma] = 0.143 \text{ keV}. \tag{16}$$

TABLE II: The mass of particle  $\eta_{c2}(1^1D_2)$  and its EM decay widths, as well as the ratios of decay widths.

	ours	[35]	[33]	[34]	[12]	[37]	[24]	[18]
$M_{(\eta_{c2}(1^1D_2))}(\text{MeV})$	3828.2	3820	3825	3811	3837(3872)	3796	3872	3820
$\Gamma(\eta_{c2}(1^1D_2) \rightarrow h_c(1P)\gamma)(\text{keV})$	284	288	303	245	344(464)	375	587 $\sim$ 786	362
$\Gamma(\eta_{c2}(1^1D_2) \rightarrow J/\psi\gamma)(\text{keV})$	1.04	0.699					3.11 $\sim$ 4.78	
$\Gamma(\eta_{c2}(1^1D_2) \rightarrow \psi(2S)\gamma)(\text{eV})$	3.08	1					17 $\sim$ 29	
$\Gamma(\eta_{c2}(1^1D_2) \rightarrow \psi(3770)\gamma)(\text{keV})$	0.143		0.34				0.49 $\sim$ 0.56	
$\frac{\Gamma(\eta_{c2}(1^1D_2) \rightarrow J/\psi\gamma)}{\Gamma(\eta_{c2}(1^1D_2) \rightarrow h_c(1P)\gamma)} \times 10^{-3}$	3.66	2.43					3.96 $\sim$ 8.14	
$\frac{\Gamma(\eta_{c2}(1^1D_2) \rightarrow \psi(2S)\gamma)}{\Gamma(\eta_{c2}(1^1D_2) \rightarrow h_c(1P)\gamma)} \times 10^{-5}$	1.08	0.347					2.16 $\sim$ 4.94	
$\frac{\Gamma(\eta_{c2}(1^1D_2) \rightarrow \psi(3770)\gamma)}{\Gamma(\eta_{c2}(1^1D_2) \rightarrow h_c(1P)\gamma)} \times 10^{-4}$	5.04		11.2				6.23 $\sim$ 9.54	

The results show that the decay width of  $\eta_{c2}(1^1D_2) \rightarrow h_c(1P)\gamma$  is more than two orders of magnitude wider than those of other channels.

For comparison, we present our results and those from other theoretical predictions in Table II. It can be seen from Table II, the predicted masses of  $\eta_{c2}(1^1D_2)$  by different models are mostly concentrated in a small range, 3796  $\sim$  3837 MeV. Some theories have attempted the possibility of a mass of 3872 MeV, mainly because they examined the possibility of the new particle  $X(3872)$  as the  $\eta_{c2}(1^1D_2)$ . Our predicted mass of  $\eta_{c2}(1^1D_2)$ , 3828.2 MeV, is very close to the masses predicted in Refs. [18, 33, 35], which are 3825 MeV and 3820 MeV, respectively.

As a electric dipole  $E1$  dominant decay, the radiative transition  $\eta_{c2}(1^1D_2) \rightarrow h_c(1P)\gamma$  is the dominant decay channel of  $\eta_{c2}(1^1D_2)$ . Other decays dominated by magnetic dipole  $M1$  transition have very small partial widths. We also show the ratios of  $\frac{\Gamma(\eta_{c2} \rightarrow \psi\gamma)}{\Gamma(\eta_{c2} \rightarrow h_c\gamma)}$  in Table II. It can be seen that the predicted widths of  $\eta_{c2}(1^1D_2) \rightarrow h_c(1P)\gamma$  from different models are comparable, except for Ref.[24] which has a much larger width, which may be due to the use of a heavier mass of  $\eta_{c2}(1^1D_2)$ . For the decay processes dominated by  $M1$  transition,  $\eta_{c2} \rightarrow \psi\gamma$ , there are significant differences between theoretical results. We believe that the main reason for this difference is the relativistic correction, which means the electric quadrupole  $E2$  transition has a significant contribution to such processes, see the next

subsection.

## B. Contribution of different partial waves in EM decay

In our method [42], the construction of the wave function is not based on the wave (i.e. the orbital angular momentum), but on the  $J^P$  quantum number of the meson. Therefore, the wave function of this meson is not a pure wave, but contains at least two types of partial waves. Among them, what people are familiar with in literature is the main wave of this particle, which generally provides the non-relativistic result. In addition, other partial waves generally contribute to the relativistic corrections.

In this subsection, we investigate carefully the contributions of different partial waves of initial and final mesons in the EM decay. The results are shown in Tables III, IV, V, and VI, where “ $2^{-+}$ ” represents the wave function of initial meson  $\eta_{c2}$ , “ $1^{--}$ ” and “ $1^{+-}$ ” represent the wave functions of final state meson  $\psi$  and  $h_c$ , respectively. “*complete*” means the complete wave function, and “*S wave*”, for example, represents only the  $S$  partial wave contribute, other partial waves are ignored. To distinguish between the initial and final states, we use the symbol “*prime*” to represent the wave of the final state. So “ $D \times S'$ ” means that the contribution to the decay width from the interaction between the  $D$ -wave in the initial state and the  $S$ -wave in the final state.

### 1. $\eta_{c2}(1^1D_2) \rightarrow h_c(1P)\gamma$

Table III shows some results of different partial waves contribute to the decay width of  $\eta_{c2}(1^1D_2) \rightarrow h_c(1P)\gamma$  (some contribution of cross terms, for example,  $(D \times P')(D \times D')$  are not listed). As can be seen from Table III, the  $D$ -wave in  $\eta_{c2}(1^1D_2)$  and  $P'$  wave in  $h_c(1P)$  are their respective dominant waves, and  $D \times P'$  provide the main non-relativistic contribution, 266 keV, to the decay width, which corresponds to the  $E1$  decay.  $F \times P'$  and  $D \times D'$  are the  $M2$  decay, their widths of 1.11 keV and 0.509 keV are much smaller than those of  $E1$  decay.  $F \times D'$  is the  $E3$  transition, its contribution of 2.29 keV is a little larger than that of  $M2$  decay.

TABLE III: Contribution of different partial waves to the decay width (keV) of  $\eta_{c2}(1^1D_2) \rightarrow h_c(1P)\gamma$ .

$\begin{array}{c} 1^{+-} \\ 2^{-+} \end{array}$	<i>complete'</i>	<i>P' wave</i>	<i>D' wave</i>
<i>complete</i>	284	240	2.28
<i>D wave</i>	259	266	0.509
<i>F wave</i>	1.01	1.11	2.29

2.  $\eta_{c2}(1^1D_2) \rightarrow J/\psi\gamma$

TABLE IV: Contribution of different partial waves to the decay width (keV) of  $\eta_{c2}(1^1D_2) \rightarrow J/\psi\gamma$ .

$\begin{array}{c} 1^{--} \\ 2^{-+} \end{array}$	<i>complete'</i>	<i>S' wave</i>	<i>P' wave</i>	<i>D' wave</i>
<i>complete</i>	1.04	0.379	1.65	0.365
<i>D wave</i>	2.81	0.284	1.65	0.112
<i>F wave</i>	1.15	0.708	0	0.0725

Table IV shows the results of different partial waves contribute to the decay width of  $\eta_{c2}(1^1D_2) \rightarrow J/\psi\gamma$ . The lowest order contribution of this process comes from the  $M1$  transition, which in our method is the non-relativistic  $D \times S'$  with a small value of 0.284 keV. The second order contribution, which is also the main relativistic correction, comes from the  $E2$  transition  $D \times P'$  and  $F \times S'$ , which contribute 1.65 keV and 0.708 keV to the decay width, respectively, significantly greater than that of the lowest order. Other relativistic corrections, the  $M3$  transition  $D \times D'$  provides a partial decay width of 0.112 keV and  $F \times P' = 0$  has no contribution, while the  $E4$  transition  $F \times D'$  gives a width of 0.0725 keV. So for the decay  $\eta_{c2}(1^1D_2) \rightarrow J/\psi\gamma$ , our relativistic method includes the contributions from transitions such as  $M1 + E2 + M3 + E4$ , with the largest contribution

coming from the  $E2$  transition.

3.  $\eta_{c2}(1^1D_2) \rightarrow \psi(2S)\gamma$

TABLE V: Contribution of different partial waves to the decay width (eV) of  $\eta_{c2}(1^1D_2) \rightarrow \psi(2S)\gamma$ .

$1^{--} \backslash 2^{-+}$	<i>complete'</i>	<i>S' wave</i>	<i>P' wave</i>	<i>D' wave</i>
<i>complete</i>	3.08	0.0401	0.223	2.49
<i>D wave</i>	1.67	0.0426	0.223	0.697
<i>F wave</i>	0.367	0.0892	0	0.552

Table V shows the results of  $\eta_{c2}(1^1D_2) \rightarrow \psi(2S)\gamma$ , where we can see that the decay width is very small, in the order of eV. The main reason is that there is a node structure in the wave function of the  $2S$  state, see the second diagram in Fig. 3, and the contributions of the wave functions before and after the nodes cancel to each other, resulting in a very small width. Meanwhile, due to the node structure, it is not easy to draw clear conclusion like we did in  $\eta_{c2}(1^1D_2) \rightarrow J/\psi\gamma$ . It can only be concluded that the contribution of decay  $\eta_{c2}(1^1D_2) \rightarrow \psi(2S)\gamma$  mainly comes from relativistic corrections.

4.  $\eta_{c2}(1^1D_2) \rightarrow \psi(3770)\gamma$

In Table VI, we show the contributions of different partial waves to the decay width of  $\eta_{c2}(1^1D_2) \rightarrow \psi(3770)\gamma$ . As can be seen from Table VI, the  $D'$ -wave in the final state  $\psi(3770)$  provides the dominant contribution, and contributions of  $P'$ -wave and  $S'$ -wave can be ignored. For  $\eta_{c2}(1^1D_2)$ , the contributions of  $D$ -wave and  $F$ -wave are almost equal. In Table VI, the lowest order contribution comes from the non-relativistic  $M1$  transition,  $D \times D'$ , with a partial width of 0.0354 keV. The second order contribution is the  $E2$  transitions  $F \times D'$  and  $D \times P'$ , and the contribution of the former is 0.0359 keV, which is similar to the contribution of the lowest order.

TABLE VI: Contribution of different partial waves to the decay width (keV) of  $\eta_{c2}(1^1D_2) \rightarrow \psi(3770)\gamma$ .

$\begin{array}{c} 1^{--} \\ \diagdown \\ 2^{-+} \end{array}$	<i>complete'</i>	<i>D' wave</i>	<i>P' wave</i>	<i>S' wave</i>
<i>complete</i>	0.143	0.142	$1.12 \times 10^{-6}$	$2.19 \times 10^{-6}$
<i>D wave</i>	0.0356	0.0354	$1.12 \times 10^{-6}$	$2.42 \times 10^{-8}$
<i>F wave</i>	0.0359	0.0359	0	$2.55 \times 10^{-6}$

### C. Discussion on the width of $\eta_{c2}(1^1D_2)$

The  $\eta_{c2}(1^1D_2)$  has not been detected in experiment, so we like to estimate the full width of  $\eta_{c2}(1^1D_2)$ . In addition to EM decay  $\eta_{c2}(1^1D_2) \rightarrow h_c(1P)\gamma$ , strong decays of  $\eta_{c2}(1^1D_2)$  are also important decay channels, which can provide sizable width. Since there is no strong decay allowed by the OZI-rule, the main strong decays of  $\eta_{c2}(1^1D_2)$  are  $\eta_{c2}(1^1D_2) \rightarrow \eta_c\pi\pi$  and  $\eta_{c2}(1^1D_2) \rightarrow gg$ . In Ref. [33], Eichten *et al.* estimated  $\Gamma(\eta_{c2}(1^1D_2) \rightarrow \eta_c\pi\pi) \approx 45$  keV. In previous paper [30], we estimated  $\Gamma(\eta_{c2}(1^1D_2) \rightarrow gg) \approx 35.6$  keV. Using these two sets of values, combined with the calculations in this article, we estimate the total width of  $\eta_{c2}(1^1D_2)$  to be

$$\Gamma(\eta_{c2}(1^1D_2)) \approx \Gamma(h_c\gamma) + \Gamma(\eta_c\pi\pi) + \Gamma(gg) + \Gamma(\psi\gamma) = 366 \text{ keV}. \quad (17)$$

In Table II, Refs.[12, 24] show us that the partial widths of EM decays are sensitive to the mass of  $\eta_{c2}(1^1D_2)$ . So when estimating the total width of  $\eta_{c2}(1^1D_2)$ , this influence should be taken into account. Therefore, we change the mass of  $\eta_{c2}(1^1D_2)$  within the range of 3800 and 3872 MeV, calculate the corresponding partial widths of the EM decays, and show the results in Figure 4.

From Figure 4, it can be seen that the partial widths of EM decays of  $\eta_{c2}(1^1D_2)$  are indeed very sensitive to its mass. Taking the dominant channel  $\eta_{c2}(1^1D_2) \rightarrow h_c(1P)\gamma$  as an example, when the mass changes from 3800 MeV to 3872 MeV, the corresponding width



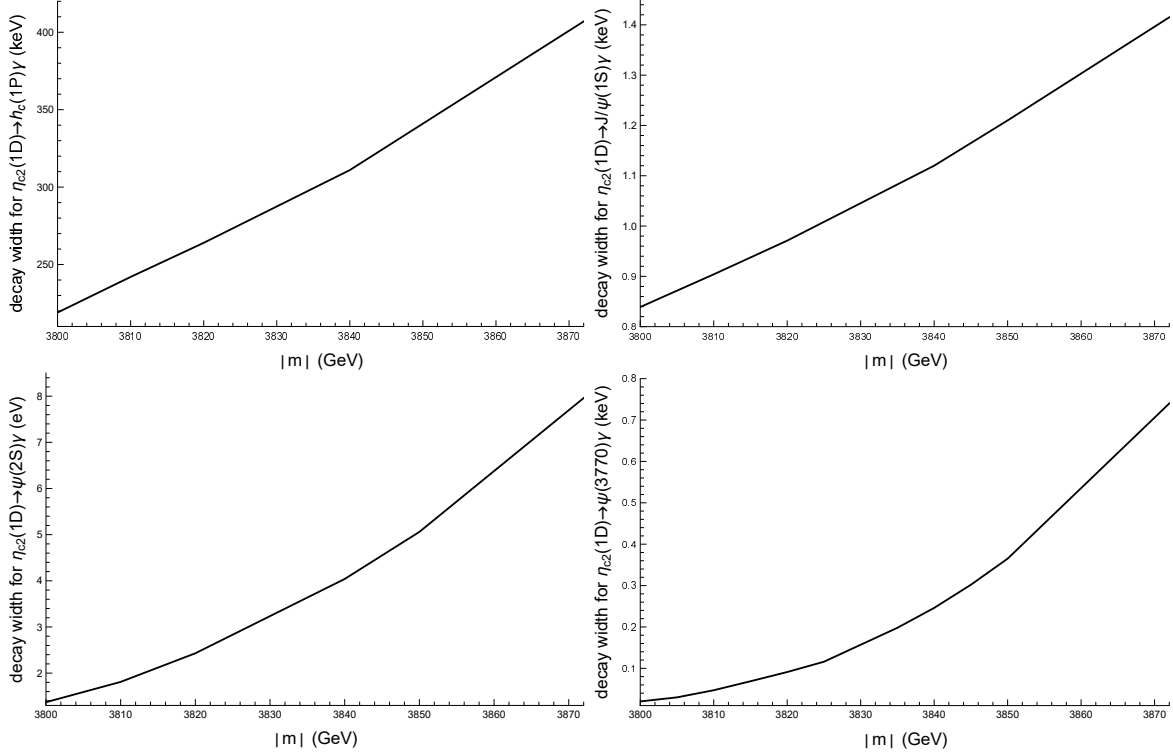


FIG. 4: The partial widths of  $\eta_{c2} \rightarrow h_c \gamma$ ,  $\eta_{c2} \rightarrow J/\psi \gamma$ ,  $\eta_{c2} \rightarrow \psi(2S) \gamma$ , and  $\eta_{c2} \rightarrow \psi(3770) \gamma$  vary along with the mass of  $\eta_{c2}$ .

changes from 220 keV to 407 keV, and their ratio is

$$\frac{\Gamma(\eta_{c2}(3800) \rightarrow h_c(1P)\gamma)}{\Gamma(\eta_{c2}(3872) \rightarrow h_c(1P)\gamma)} = 0.541.$$

Because there are no node structures in the wave functions of initial and final states, this result is purely caused by phase space. Eq.(11) shows the transition amplitude of  $\eta_{c2}(1^1D_2) \rightarrow h_c(1P)\gamma$ , where the  $2\epsilon^{\xi\epsilon_f} s_\gamma$  term gives the largest contribution. When calculating the square of the amplitude, its power of momentum  $|\vec{P}_f|$  is 4, so we roughly have

$$\frac{\Gamma(\eta_{c2}(3800) \rightarrow h_c(1P)\gamma)}{\Gamma(\eta_{c2}(3872) \rightarrow h_c(1P)\gamma)} \propto \frac{|\vec{P}_{f3800}|^5}{|\vec{P}_{f3872}|^5} = 0.459,$$

this estimate is very close to our calculated value of 0.541.

## IV. CONCLUSION

In this paper, by constructing the general relativistic wave function for the  $2^-$  state according to its quantum number of  $J^P$  and solving the complete Salpeter equation of the  $2^-$  state, we obtain the mass of  $\eta_{c2}(^1D_2)$  is 3828.2 MeV, and the decay widths:  $\Gamma[\eta_{c2} \rightarrow h_c\gamma] = 284$  keV,  $\Gamma[\eta_{c2} \rightarrow J/\psi\gamma] = 1.04$  keV,  $\Gamma[\eta_{c2} \rightarrow \psi(2S)\gamma] = 3.08$  eV, and  $\Gamma[\eta_{c2} \rightarrow \psi(3770)\gamma] = 0.143$  keV. The full width of  $\eta_{c2}(^1D_2)$  is also estimated and a narrow width of 366 keV is obtained. We find that the partial width of its EM decay strongly depends on the mass of  $\eta_{c2}(^1D_2)$ .

We also study the contributions of different partial waves which are the non-relativistic and relativistic terms in the EM decays of  $\eta_{c2}$ . For the decay  $\eta_{c2} \rightarrow h_c\gamma$ , the main contribution comes from the non-relativistic dominant partial waves, providing the  $E1$  decay, and our calculation includes the contribution of transitions  $E1 + M2 + E3$ . For transition  $\eta_{c2} \rightarrow \psi\gamma$ , our calculation includes  $M1 + E2 + M3 + E4$  transitions, and the relativistic  $E2$  transition usually provides the main contribution.

**Acknowledgments** This work was supported in part by the National Natural Science Foundation of China (NSFC) under the Grants Nos. 12075073, 12375085, 12005169. It is also supported by the Natural Science Basic Research Program of Shaanxi (Program no. 2021JQ-074), and the Fundamental Research Funds for the Central Universities.

- 
- [1] S.K. Choi *et al.* (Belle Collaboration), Phys. Rev. Lett. **91**, 262001 (2003).
  - [2] S. Uehara *et al.* (Belle Collaboration), Phys. Rev. Lett. **96**, 082003 (2006).
  - [3] B. Aubert *et al.* (BaBar Collaboration), Phys. Rev. D **81**, 092003 (2010).
  - [4] J.P. Lees *et al.* (BaBar Collaboration), Phys. Rev. D **86**, 072002 (2012).
  - [5] K. Chilikin *et al.* (Belle Collaboration), Phys. Rev. D **95**, 112003 (2017).
  - [6] Kazuo Abe *et al.* (Belle Collaboration), Phys. Rev. Lett. **98**, 082001 (2007).
  - [7] P. Pakhlov *et al.* (Belle Collaboration), Phys. Rev. Lett. **100**, 202001 (2008).
  - [8] Bernard Aubert *et al.* (BaBar Collaboration), Phys. Rev. Lett. **95**, 142001 (2005).
  - [9] M. Ablikim *et al.* (BESIII Collaboration), Phys. Rev. Lett. **110**, 252001 (2013).

- [10] Medina Ablikim *et al.* (BESIII Collaboration), Phys. Rev. Lett. **126**, 10, 102001 (2021).
- [11] S. Godfrey, Nathan Isgur, Phys. Rev. D **32**, 189 (1985).
- [12] T. Barnes, S. Godfrey, and E.S. Swanson, Phys. Rev. D **72**, 054026 (2005).
- [13] Petros A. Rapidis, B. Gobbi, D. Luke, Angela Barbaro-Galtieri, J. Dorfan *et al.* Phys. Rev. Lett. **39**, 526 (1977).
- [14] V. Bhardwaj *et al.* (Belle Collaboration), Phys. Rev. Lett. **111**, 3, 032001 (2013).
- [15] M. Ablikim *et al.* (BESIII Collaboration), Phys. Rev. Lett. **115**, 1, 011803 (2015).
- [16] Wei Li, Su-Yan Pei, Tianhong Wang, Ying-Long Wang, Tai-Fu Feng, Guo-li Wang, Phys. Rev. D **107**, 113002 (2023).
- [17] Ning Li, Yan Hao, Feiyu Chen, Ying Chen, Xiangyu Jiang, Chunjiang Shi, Wei Sun, Phys. Rev. D **109**, 014513 (2024).
- [18] Wei-Jun Deng, Hui Liu, Long-Cheng Gui, and Xian-Hui Zhong, Phys. Rev. D **95**, 3, 034026 (2017).
- [19] Wei Li, Su-Yan Pei, Tianhong Wang, Tai-Fu Feng, Guo-li Wang, Phys. Rev. D **109**, 036011 (2024).
- [20] Guo-Liang Yu, and Zhi-Gang Wang, Int. J. Mod. Phys. A **34**, 1950151 (2019).
- [21] R. Aaij *et al.* (LHCb Collaboration), JHEP **07**, 035 (2019).
- [22] Yu. S. Kalashnikova, A. V. Nefediev, Phys. Rev. D **82**, 097502 (2010).
- [23] Hong-Wei Ke, and Xue-Qian Li, Phys. Rev. D **84**, 114026 (2011).
- [24] Yu Jia, Wen-Long Sang, and Jia Xu, arXiv: 1007.4541v1 [hep-ph].
- [25] R. Aaij *et al.* (LHCb Collaboration), Phys. Rev. Lett. **110**, 222001 (2013).
- [26] Roel AaijZ *et al.* (LHCb Collaboration), Phys. Rev. D **92**, 1, 011102 (2015).
- [27] K. Chilikin *et al.* (Belle Collaboration), JHEP **05**, 034 (2020).
- [28] S. Jia *et al.* (Belle Collaboration), Phys. Rev. D **104**, 012012 (2021).
- [29] Li Yang, Wen-Long Sang, Hong-Fei Zhang, Yu-Dong Zhang, and Ming-Zhen Zhou, Phys. Rev. D **103**, 3, 034018 (2021).
- [30] Tianhong Wang, Guo-Li Wang, Wan-Li Ju, Yue Jiang, JHEP **03**, 110 (2013).
- [31] V.A. Novikov, L.B. Okun, Mikhail A. Shifman, A.I. Vainshtein, M.B. Voloshin *et al.* Phys.Rept. **41**, 1 (1978).

- [32] Ying Fan, Zhi-Guo He, Yan-Qing Ma, and Kuang-Ta Chao, Phys. Rev. D **80**, 014001 (2009).
- [33] Estia J. Eichten, Kenneth Lane, and Chris Quigg, Phys. Rev. Lett. **89**, 162002 (2002).
- [34] D. Ebert, R.N. Faustov, and V.O. Galkin, Phys. Rev. D **67**, 014027 (2003).
- [35] K.J. Sebastian, and X.G. Zhang, Phys. Rev. D **55**, 225 (1997).
- [36] Yi-Bo Yang *et al.* (CLQCD Collaboration), Phys. Rev. D **87**, 1, 014501 (2013).
- [37] Bai-Qing Li, and Kuang-Ta Chao, Phys. Rev. D **79**, 094004 (2009).
- [38] Peng Guo, Tochtli Yépez-Martínez, and Adam P. Szczepaniak, Phys. Rev. D **89**, 11, 116005 (2014).
- [39] G.-L. Wang, T.-F. Feng, X.-G. Wu, Phys. Rev. D **101**, 116011 (2020).
- [40] E.E. Salpeter, and H.A. Bethe, Phys. Rev. **84**, 1232 (1951).
- [41] E.E. Salpeter, Phys. Rev. **87**, 328 (1952).
- [42] Guo-Li Wang, Tianghong Wang, Qiang Li, and Chao-Hsi Chang, JHEP **05**, 006 (2022).
- [43] G.-L. Wang, Q. Li, T. Wang, T.-F. Feng, X.-G. Wu, and C.-H. Chang, Eur. Phys. J. C **82**, 1027 (2022).
- [44] T.-H. Wang, and G.-L. Wang, Phys. Lett. B **697**, 233 (2011).
- [45] T.-H. Wang, Y. Jiang, W.-L. Ju, H. Yuan, and G.-L. Wang, JHEP **03**, 209 (2016).
- [46] Su-Yan Pei, Wei Li, Ting-Ting Liu, Meng Han, Guo-li Wang, Tian-Hong Wang, Phys. Rev. D **108**, 033003 (2023).
- [47] Chao-Hsi Chang, Jiao-Kai Chen, and Guo-Li Wang, Commun. Theor. Phys. **46**, 467 (2006).
- [48] C.S. Kim, and Guo-Li Wang, Phys. Lett. B **584**, 285 (2004); Phys. Lett. B **634**, 564 (2006) (erratum).
- [49] G.-L. Wang, Phys. Lett. B **633**, 492 (2006).
- [50] Chao-Hsi Chang, and Guo-Li Wang, Sci. China Phys. Mech. Astron. **53**, 2005 (2010).
- [51] Zhi-Hui Wang, Guo-Li Wang, Hui-Feng Fu, and Yue Jiang, Phys. Lett. B **706**, 389 (2012).